Journal of Materials Chemistry C

Accepted Manuscript

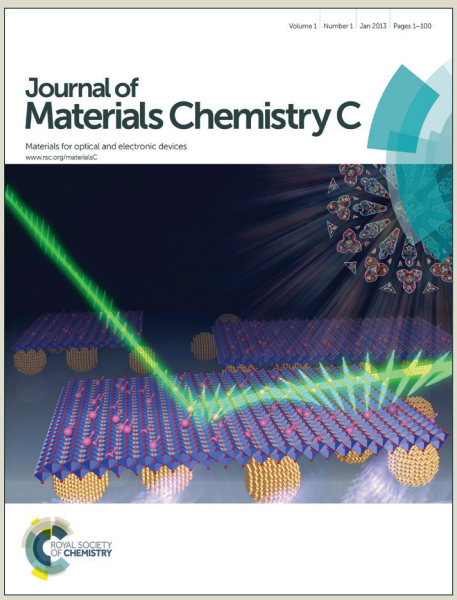

ROYAL SOCIETY OF CHEMISTRY

www.rsc.org/materialsC

Journal Name

RSCPublishing

ARTICLE

Simultaneous ROMP and Titania Sol-Gel Reactions and Nanodispersed Functional Organic-Inorganic Composite Hybrid Materials

Johannes A. van Hensbergen,[a] Meina Liu,[a] Robert P. Burford*[a] and Andrew B. Lowe*[a]

Cite this: DOI: 10.1039/xoxxoooooox

Received ooth January 2012,
Accepted ooth January 2012

DOI: 10.1039/xoxxoooooox

www.rsc.org/

This contribution addresses the important issue of chemical, kinetic and thermodynamic matching in the one-pot preparation of organic-inorganic hybrid materials based on ***simultaneous*** titania sol-gel chemistry and ring-opening metathesis polymerization (ROMP). Few systems are amenable to concurrent and *in situ* sol-gel/polymerization processes, but the rapid rate and functional group tolerance of Grubbs' catalyst mediated ROMP impart ideal kinetic and chemical compatibility with β-diketone moderated sol-gel condensation. Hybrids containing targeted loadings of up to 20 wt% TiO_2 nanoparticles, evenly dispersed throughout the organic matrix, were prepared with commercially available norbornene as well as a range of functional *exo*-7-oxanorbornenes synthesized via thiol-Michael coupling chemistry. The thermodynamic compatibility of these systems was further improved via the use of a novel triethoxysilane functionalized monomer to introduce strong C-Si-O-Ti- bonds between the organic and inorganic phases. The resulting covalently bound hybrids were molecularly homogeneous, optically transparent, orange in colour and behaved as acid degradable thermosets. Significantly, they could incorporate up to 75 wt% of Ti-based species (without phase separation), as well as various hydrophobic and functional comonomers for additional versatility and the modification of physical properties. Raman analysis suggested the Ti existed in an amorphous state while TGA analysis implied the presence of Ti-hydrates.

Introduction

Organic-inorganic (nano)composites (OINCs) are an increasingly attractive class of materials that have been employed in a wide range of novel applications, including: optics, energy and solar cells, adjustable band-gap electronics,[1] and next generation, lightweight, long-life, environmentally friendly materials with enhanced thermal, mechanical and barrier properties.[2-10] Traditionally, such hybrids are prepared by dispersing preformed inorganic particles, porous clusters or exfoliated layers in a molten or dissolved polymer.

In the preparation of OINCs, optimal homogeneity is attained when the formation of the organic and inorganic phases are performed *in situ* and simultaneously.[11] Unfortunately, the high temperature solid state reactions typically employed to prepare inorganics are incompatible with organic polymers which begin to degrade above 250 °C. To circumvent this, the sol-gel polycondensation process is commonly employed.[4, 11-14] Metal alkoxide or halide precursors, such as tetraethylorthosilicate (TEOS) for silica-based or $TiCl_4$ for titania-based systems, are hydrolysed followed by a condensation process to yield a metal oxide framework at ambient temperature under non-demanding experimental conditions.

The sol-gel process is a convenient method to circumvent the high temperature approach to inorganic phase preparation. However, when preparing OINCs ***concurrently*** the individual chemical processes must be chemically, kinetically and thermodynamically compatible to prevent macroscopic phase separation. As an example, sol-gel reactions liberate alcohols during the polycondensation reaction sequence, and are incompatible with any polymerization process sensitive to alcohols, such as a living anionic polymerization. Therefore, while a sol-gel/anionic polymerization combination may be compatible *sequentially*, it is inherently incompatible simultaneously (without even considering associated kinetics or thermodynamics). This is an extremely important consideration and, so, the majority of hybrid materials are prepared ***sequentially***.[7, 15-41] Kickelbick highlights such important compatibility considerations in his reviews[4, 11] and he, and others, offer various examples. For instance, Donescu *et al.* were unable to perform *in situ* radical polymerisation of vinyl acetate derived monomers in the presence of Ti-based sol-gel

precursors due to changes in the valence of the Ti atoms and the occurrence of redox processes. Similarly, Brusatin and Giustina[42] note considerable difficulty in preserving epoxide functionality during simultaneous ring-opening polymerisation and sol-gel condensation due to the strong Lewis acid behaviour of titania systems.

Ring-opening metathesis polymerization (ROMP) is a transition metal-mediated process that can yield (co)polymers with predetermined molecular weights, low dispersities ($Đ_M = \bar{M}_w/\bar{M}_n$), and advanced architecture (co)polymers for use in a range of novel applications.[43-52] When considering the design of systems amenable to simultaneous sol-gel/polymerisation formulations, the rapid, facile preparation of (co)polymers via ROMP containing a broad range of functionality and physical properties would appear to render ROMP-prepared materials perfect for application in OINC syntheses. Surprisingly however, ROMP as a synthetic tool for the organic phase has been largely overlooked.

To the best of our knowledge there are only a handful of reports in the open literature in which ROMP has been combined with sol-gel chemistry. Ellsworth and Novak[53] reported concurrent hybrid systems with a series of simple functional oxanorbornenes in aqueous media employing poorly defined Ru-catalysts ($Ru(H_2O)_6(tos)_2$ for example) with a ***silica***-based sol-gel process to give homogeneously dispersed hybrid materials. The authors also extended the work to include an alkoxysilane ROMP-active monomer to improve compatibility and minimize polymerisation-associated shrinkage. More recently, Kir and co-workers[54] reported a ***sequential*** process in which ROMP-prepared block copolymers containing carboxylic acid and TEMPO functional side groups were first prepared. The block copolymers were then reacted with $TiCl_4$ in MeOH for three days, ultimately resulting in the formation of a gel with C-O-Ti bonds between the inorganic TiO_2 domains and the organic polymer. After drying, the composite materials were characterized via a combination of small angle X-ray scattering and X-ray diffraction.

We have recently been examining metathesis-based polymerisation processes to prepare new and interesting linear and non-linear macromolecules.[55-61] Expanding on our recent research efforts we herein detail the first examples of *simultaneous* titania-based sol-gel/ROMP formulations employing a *well-defined* Ru Grubbs catalyst to give new titania-based nanomaterials.[62] We also demonstrate the *concurrent* preparation of new hybrid materials containing covalently linked organic and inorganic domains via the proposed formation of C-Si-O-Ti-O bonds giving novel silica-titania-organic hybrid materials. Such formulations are applicable to simple ROMP-active substrates as well as highly functional *exo*-7-oxanorbornene derivatives such as the thioether derivatives we reported recently, giving a whole new family of functional OINCs.

Experimental

All reagents were purchased from the Aldrich Chemical Company and Hybrid Plastics Inc. at the highest available purity and used as received unless stated otherwise.

Instrumentation

FTIR Spectroscopy

Infrared spectra were collected in a Thermo Nicolet 5700 FTIR spectrometer equipped with a single bounce diamond stage attenuated total reflectance (ATR) accessory. A resolution of 2 cm^{-1} and a spectral window of 650 to 4000 wavenumbers was chosen and spectra were accumulated from 32 averaged scans.

Raman SPECTROSCOPY

Raman spectra were collected on a spectrometer with 514 nm excitation (argon ion laser) with an 1800 l/mm grating. Samples were focussed to a ~ 1.5 micron spot employing a 50x objective. The laser power was dropped to 5-10% maximum power (10.6 mW) to reduce observed fluorescence and laser damage.

Scanning electron microscopy

Scanning electron microscopy (SEM) of etched hybrid materials was carried out in a Hitachi S3400 instrument in high vacuum mode. Samples were completely submerged in a Teflon® beaker containing an aqueous solution of 48 wt% hydrofluoric acid. After 4 h., the samples were removed and rinsed with water before being placed in a vacuum oven (3 days, oven temperature = 40 °C, residual pressure = 15 kPa). Dried samples were mounted on brass stubs using double sided carbon tape and coated for conductivity with an Emitech K550x Gold Sputter Coater. A probe current of 10 μA and an accelerating voltage of 30 kV were typically employed for imaging.

Transmission electron microscopy

Transmission electron microscopy (TEM) of hybrid samples was performed in a JEOL 1400 transmission electron microscope. Thin (ca. 100 nm) representative sections were cut from liquid nitrogen cooled hybrids using a Leica FC6 cryo-ultramicrotome and, mounted on copper grids. Staining was not necessary due to sufficient atomic contrast between titania (TiO_2) and the organic polymer phase and all samples were loaded and imaged directly. An emission current of 80 μA and an accelerating voltage of 100 kV were selected.

Thermogravimetric analysis

The thermal stability, degradation behavior and inorganic loading of hybrid samples were determined with a TA instruments Q5000 Hi-Res thermogravimetric analyzer (TGA). The instrument was operated under air for all samples with a nominal flow rate of 60 cm^3/ min. Samples (ca. 40.0 mg) were added to ceramic reinforced Pt pans and heated to 1000 °C at 20 °C/min, with a 10 min. isothermal step at 120 °C to remove

residual solvent and absorbed water. Mass loss was recorded as a function of temperature and derivative traces were computed.

Dynamic mechanical analysis

Hybrid samples were prepared and cured in a silicone rubber mould to obtain uniform rectangular (30 x 6 x 2 mm) test bars for dynamic mechanical analysis (DMA). After drying in a vacuum oven, the test bars were loaded into a single cantilever clamp on a TA Instruments Q800 dynamic mechanical analyser. The sample chamber was cooled to an initial temperature of -50 °C with a liquid nitrogen gas cooling accessory (GCA) and a oscillatory force was applied to maintain a frequency of 1 Hz and a deformation of 20 μm. Samples were heated to 100 °C at 5 °C/min and storage modulus, loss modulus and tan delta were calculated as a function of temperature.

Small angle X-ray scattering

Small angle x-ray scattering (SAXS) data was collected on a NanoSTAR II SAXS instrument (Bruker AXS, Karlsruhe). The X-ray source (copper rotating anode 0.3 mm filament) was operated at 45 kV and 110 mA (Cu Kα radiation wavelength, λ = 1.5418 Å) and the instrument was fitted with Montel multilayer optics and three pin-hole collimation for point focus geometry (750 μm source; 400 μm; 1000 μm diameter pinholes).[63] A 1.0 mm diameter FWHM beam was used at the sample position. A Vantec 2D detector (2048 x 2048 pixels; pixel size 68 x 68 μm^2) was located centrally about the beam axis, and a 2.85 mm diameter beamstop was placed immediately in front of the detector. The sample to detector distance was calibrated using a standard sample (silver behenate powder) and measured as 71.25 mm. Samples were mounted on a multi-position X-Y translation stage and aligned with the X-ray beam using a sample absorption scan (reproducible to better than 0.01 mm). Optics and sample chambers were kept under vacuum to minimize background associated with air scatter. For each sample the 2D SAXS data was collected for 3600 s. as a function of scattering vector Q over the range $0.011 < Q < 0.39$ $Å^{-1}$. The 2D data was corrected for detector spatial effects and variation in sensitivity, and reduced to 1D data using Bruker software. All data was corrected for variation in sample thickness using the sample transmission for normalization.

Syntheses

Monomer synthesis

All functional *exo*-7-oxanorbornene monomers (Figure 1) were synthesized via previously reported procedures.[55] Monomers included:

M1: (3a*R*,7a*S*)-2-butyl-3a,4,7,7a-tetrahydro-1*H*-4,7-epoxy isoindole-1,3(2*H*)-dione; **M2:** (3a*R*,7a*S*)-2-ethyl-3a,4,7,7a-tetrahydro-1*H*-4,7-epoxyisoindole-1,3(2*H*)-dione; **M3:** 2-((3a*R*,7a*S*)-1,3-dioxo-1,3,3a,4,7,7a-hexahydro-2*H*-4,7-epoxy-isoindol-2-yl)ethyl 3-((2-hydroxyethyl)thio)propanoate; **M4:** 2-((3a*R*,7a*S*)-1,3-dioxo-1,3,3a,4,7,7a-hexahydro-2*H*-4,7-epoxy-isoindol-2-yl)ethyl 3-((2,3-dihydroxypropyl)thio)prop-anoate; **M5:** (2*S*,3*S*,4*S*,5*R*,6*R*)-6-((3-(2-((3a*R*,7a*S*)-1,3-dioxo-1,3,3a,4,-7,7a-hexahydro-2*H*-4,7-epoxyisoindol-2-yl)ethoxy)-3-oxo-propyl)thio)tetrahydro-2*H*-pyran-2,3,4,5-tetrayl tetraacetate; **M6:** *N*-(3-((3a*R*,7a*S*)-1,3-dioxo-1,3,3a,4,7,7a-hexahydro-2*H*-4,7-epoxyisoindol-2-yl)propyl)-*N*,*N*-dimethylbutan-1-ammonium bromide; **M7:** 2-((3a*R*,7a*S*)-1,3-dioxo-1,3,3a,4,7,7a-hexahydro-2*H*-4,7-epoxyisoindol-2-yl)ethyl 3-(dodecylthio)propanoate; **M8:** 2-((3a*R*,7a*S*)-1,3-dioxo-1,3,3a,4,7,7a-hexahydro-2*H*-4,7-epoxyisoindol-2-yl)ethyl 3-(benzyl thio)propanoate; **M9:** 2-((3a*R*,7a*S*)-1,3-dioxo-1,3,3a,4,7,7a-hexahydro-2*H*-4,7-epoxyisoindol-2-yl)ethyl 3-((4,5-dihydrothia-zol-2-yl)thio)propanoate; **M10:** methyl ((2*S*)-3-((3-(2-((3a*R*,7a*S*)-1,3-dioxo-1,3,3a,4,7,7a-hexahydro-2*H*-4,7-epoxyiso-indol-2-yl)ethoxy)-3-oxopropyl)thio)-2-methylpropanoyl)-*L*-prolinate; **M11:** 2-((3a*R*,7a*S*)-1,3-dioxo-1,3,3a,4,7,7a-hexahydro-2*H*-4,7-epoxyisoindol-2-yl)ethyl 3-((4,4,5,5,6,6,7,7,8,8,9,9,10,10,11,11,11-heptadecafluoroundecyl)thio)propanoate; **TES:** 2-((3a*R*,7a*S*)-1,3-dioxo-3a,4,7,7a-tetrahydro-1*H*-4,7-epoxyisoindol-2(3*H*)-yl)ethyl 3-((3-(triethoxysilyl)propyl)thio)propanoate; **POSS1:** NB1022 Norbornenylethylisobutyl POSS(R) – Hybrid Plastics Inc.; **POSS2:** NB1038 Norbornenylethyldisilanolisobutyl POSS(R) – Hybrid Plastics Inc.

Polynorbornene/TiO_2 hybrid synthesis

Norbornene (4.5 g, 48.0 mmol) was added to a glass vial and dissolved in CH_2Cl_2 (1.0 mL). Titanium isopropoxide (1.85 mL, with the potential to form 0.5 g of TiO_2) was added and the mixture cooled to just above its freezing point in liquid N_2. A solution of 2nd generation (**G2**) Grubbs catalyst (1,3-bis(2,4,6-trimethylphenyl)-2-imidazolidinylidene)dichloro(phenyl methylene)(tricyclohexylphosphine)ruthenium) (1.0 mg, 0.0025 mol%) in CH_2Cl_2 (0.5 mL) was added and the reaction stirred vigorously until homogeneous. The mixture was then transferred to a suitable mould and covered with a glass petri dish to prevent premature evaporation of solvent. As the mixture absorbed moisture from the air and the mould increased in temperature, the hydrolysis/condensation and ring-opening metathesis polymerisations proceeded, yielding a solid opaque white material. The hybrid was then dried for 72 h. in a vacuum oven to remove residual solvent and isopropanol. Alternative TiO_2 loadings were achieved by varying the ratio of monomer to titanium isopropoxide.

Polynorbornene and functional *exo*-7-oxanorbornene/TiO_2 hybrid preparation with acetylacetone

A pre-sol of stabilized TiO_2 nanoparticles was prepared by adding titanium isopropoxide (5.0 mL with the potential to form 1.35 g and 16.9 mmol of TiO_2) directly into acetylacetone (3.0 mL, 29.2 mmol, 1.7 eq.), followed by 0.5 mL of a 1:1 H_2O/HCl solution. This pre-sol was then concentrated *in vacuo* until there was no further observable change in volume to

remove the majority of isopropanol leaving groups generated by the hydrolysis reactions. A portion of the concentrated pre-sol (37 % by volume or ca. 1-2 mL) was then added to a solution of norbornene (4.5 g, 48.0 mmol) or functional *exo*-7-oxanorbornene monomer (4.5 g) in CH_2Cl_2 (1.0 mL). The mixture was cooled to just above its freezing point in liquid N_2 before Grubbs **G2** catalyst (1.0 mg, 0.0025 mol%) in CH_2Cl_2 (0.5 mL), was injected. The reaction was stirred vigorously until homogeneous and then transferred to a covered mould as previously described. As the mixture heated, the ring-opening metathesis polymerisation proceeded to high conversion and yielded an orange translucent material. The hybrid was dried for 72 h. in a vacuum oven (oven temperature = 40 °C, residual pressure = 15 kPa) to remove residual solvent and isopropanol. Alternative TiO_2 loadings were obtained by varying the ratio of monomer to pre-sol.

Preparation of covalently bound functional *exo*-7-oxanorbornene/TiO_2 hybrids

A pre-sol of TiO_2 covalently bound to monomer was prepared by adding titanium isopropoxide (60 µL), with the potential to form 0.02g and 0.25 mmol of TiO_2) directly into 2-((3a*R*,7a*S*)-1,3-dioxo-3a,4,7,7a-tetrahydro-1*H*-4,7-epoxyiso indol-2(3*H*)-yl)ethyl 3-((3-(triethoxysilyl)propyl)thio) propanoate (**TES**) (0.18 g, 0.36 mmol). After several minutes, acetylacetone (35 µL, 0.42 mmol) was also added, followed by 5 µL of a 1:1 H_2O/ HCl solution. The pre-sol was concentrated *in vacuo* to remove the majority of isopropanol leaving groups generated by the hydrolysis reactions, and then cooled to just above its freezing point in liquid N_2. G2 Grubbs' catalyst (1.0 mg, 0.33 mol%) in CH_2Cl_2 (100 µL) was injected and the reaction stirred vigorously until homogeneous before being transferred to a covered mould. As the mixture heated, ROMP proceeded to high conversion and yielded an orange, optically transparent material that was dried for 72 h. in a vacuum oven (oven temperature = 40 °C, residual pressure = 15 kPa). Alternative TiO_2 loadings (20, 30, 40, 50 and 75 wt%) were achieved by varying the ratio of triethoxy monomer (**TES**) to titanium isopropoxide. Functional copolymers were also prepared as the organic phase by substituting varying amounts (50, 75 and 90 mol%) of the triethoxy monomer (**TES**) for a different functional *exo*-7-oxanorbornene.

Results and Discussion

In determining suitable formulations allowing for concurrent titania-based sol-gel polycondensation with chain growth ROMP polymerization we first examined the simple monomer norbornene (**NBE**, Figure 1). The TiO_2 precursor, titanium isopropoxide (TIP), was insoluble in norbornene but the addition of an appropriate compatibilizing solvent such as CH_2Cl_2 allowed for the preparation of three polynorbornene (PNBE) based composites containing 10, 20 and 50 wt% Ti species. While these materials were not transparent, suggesting an inherent incompatibility between the organic and inorganic phases, we evaluated the physical properties to confirm the validity of the approach for preparing materials with tuneable physical properties. Characterization of samples by TGA and DMA, Figure 2A and B, confirmed that the target inorganic loadings had been achieved while the DMA results revealed that the inclusion of the inorganic Ti component increased the resulting composites' T_g by an amount proportional to the titania loading (note: the 50 wt% sample was too brittle to be mounted on the instrument and therefore was not analysed).

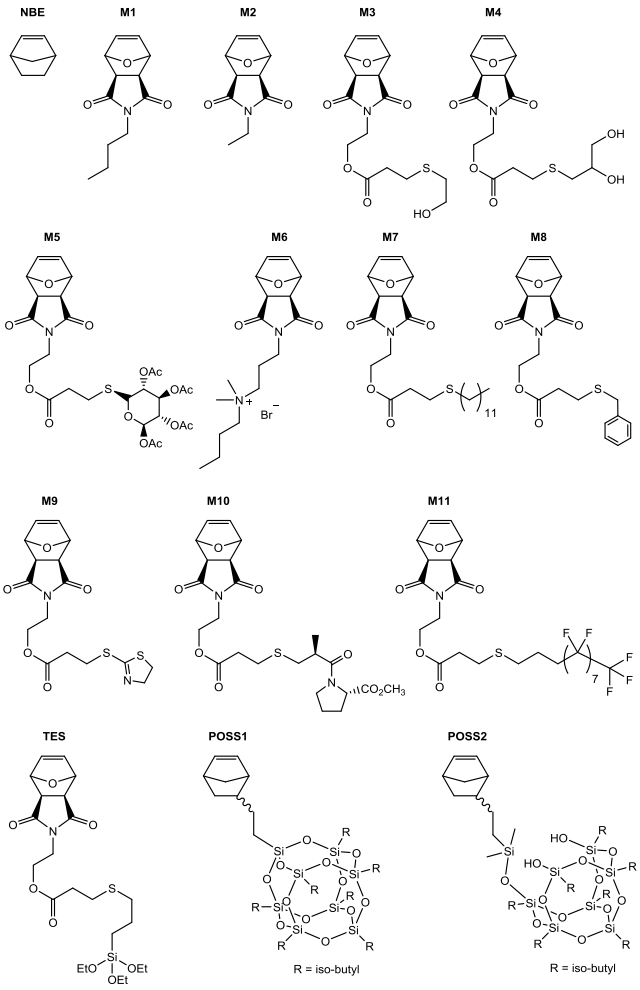

Figure 1. Chemical structures of the (oxa)norbornene-based, ROMP-active, monomers employed in the evaluation of simultaneous titania-based sol-gel and ring-opening metathesis polymerisation processes.

We also note that the initial weight loss observed in the TGA suggests the formation of oligomeric/polymeric Ti-OH species, as opposed to pure TiO_2, due to incomplete condensation reactions.

While these preliminary experiments were successful in validating the compatibility of simultaneous *in-situ* ROMP with titania sol-gel chemistry, additional SEM characterization indicated that these materials were not optimal. Although energy dispersive X-ray spectroscopy (EDS) qualitatively confirmed the presence of the inorganic component, SEM images of pyrolysis chars and samples where the inorganic

phase had been selectively etched away with HF (see supporting information) revealed that the inorganic domains were large (micrometre scale) and non-uniform. Such morphologies are indicative of phase separation/agglomeration or an excessively rapid and uncontrolled sol-gel condensation, i.e. a kinetic mismatch.

To improve the homogeneity of the targeted ROMP/titania sol-gel hybrids we evaluated the use of acetylacetone (AcAc). The hydrolysis and condensation of species such as TIP proceeds rapidly and it is common to employ bidentate ligands such as AcAc, or other β-diketones, as moderators to control (reduce) the polycondensation kinetics.[4] By competitively coordinating with TIP, the enol of AcAc effectively slows the rate of condensation reactions and stabilizes the resulting Ti-based species.[64, 65] Three additional PNBE/Ti hybrids (at 10, 20 and 50 wt% loading) each containing 1.7 equivalents of AcAc were prepared and characterized. While the 20 and 50 wt% samples were opaque the 10 wt% TiO_2 hybrid was semi-translucent suggesting that its inorganic domains were well dispersed and approaching nano-scale dimensions. SEM images of the HF etched hybrids and pyrolysis chars of the 10 wt% sample confirmed that the inorganic phase was restricted to discrete, well-dispersed particles in the size range 100-200 nm, Figure 3, while the 20 and 50 wt% hybrids contained a mixture of dispersed nanoparticles and larger aggregates (see supporting information).

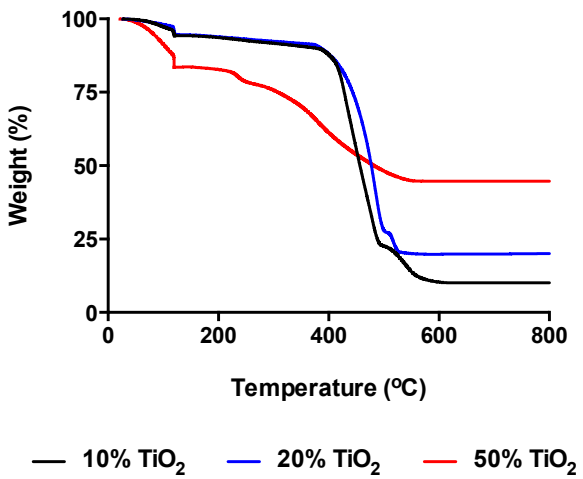

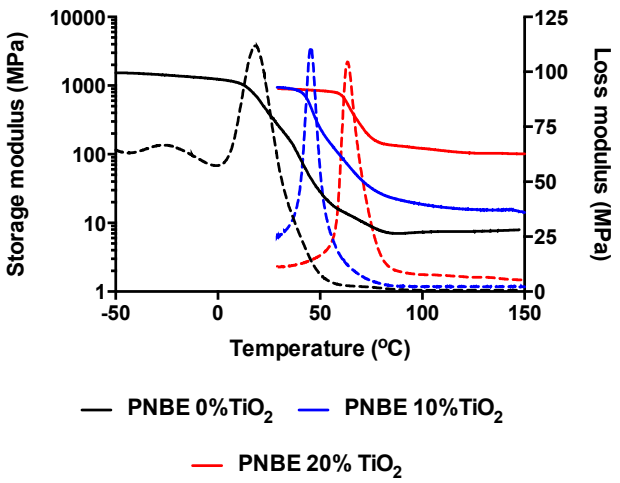

Figure 2. (A) TGA traces of a PNBE control and 10, 20 and 50 wt% Ti-based composites confirming target inorganic loadings; (B) dynamic mechanical analyses (DMA) for PNBE/Ti-based composites highlighting the increase in glass transition temperature with inorganic content.

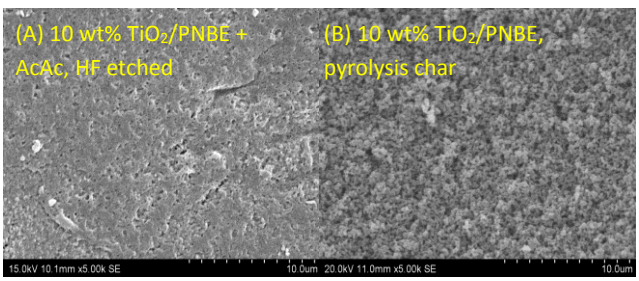

Figure 3. (A) SEM image of HF etched PNBE/Ti-based 10 wt% composite prepared with AcAc as a compatibilizing agent, demonstrating the well-dispersed nanometre scale of the inorganic phase; (B) pyrolysis char of the same sample also highlighting the nanometre nature of the residual TiO_2.

Although the application of AcAc as a chelating agent did not completely prevent phase separation, especially at higher weight loadings of titania, it is noted that there are a large number of commercially available β-diketones bearing a wide-range of functionality that may serve as better compatibilizing agents with the hydrophobic polynorbornene matrix that could be examined.[66] We also note that these results qualitatively confirm an acceptable kinetic match between the ROMP polymerisation with the Grubbs' second-generation catalyst and the TIP-based sol-gel reaction in the presence of AcAc.

In an effort to further enhance the compatibility of the organic and inorganic phases we employed more polar metathesis-active monomers. While a metal alkoxide may exhibit a high initial affinity for an organic monomer/polymer such as NBE/PNBE, the presence of OH groups on the hydrolysed metal oxide imparts a strong hydrophilic character and ultimately a tendency to phase separate. Recently, we have been interested in the synthesis of novel functional ROMP-active *exo*-7-oxanorbornene monomers and have detailed the synthesis and polymerization of a series of novel thioether-based monomers obtained via facile thiol-Michael coupling.[55]

A selection of these monomers (Figure 1) was synthesized and trialled in the preparation of simultaneous ROMP/sol-gel hybrids.

Simply substituting **NBE** for the butyl functional *exo*-7-oxanorbornene **M1**, Figure 1, was found to increase compatibility sufficiently such that a 10 wt% Ti-based hybrid remained optically transparent and showed no macroscopic signs of phase separation. SEM analysis of this material before and after HF etching revealed that the inorganic phase existed as discrete nanoparticles with an average size < 50.0 nm, homogeneously dispersed throughout the organic matrix, Figure 4. This morphology was confirmed via TEM on cryo-microtomed sections, Figure 5.

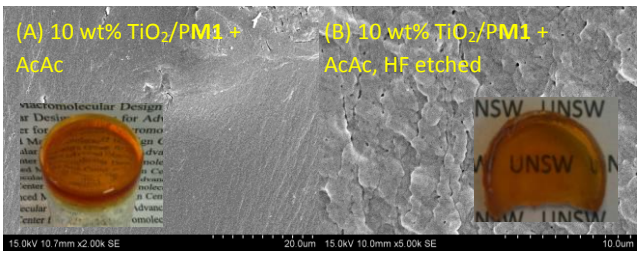

Figure 4. (A) Unetched SEM image of a 10 wt% Ti-based/**PM1** composite with inset photo showing the translucent nature of the composite; (B) the same sample after etching with HF.

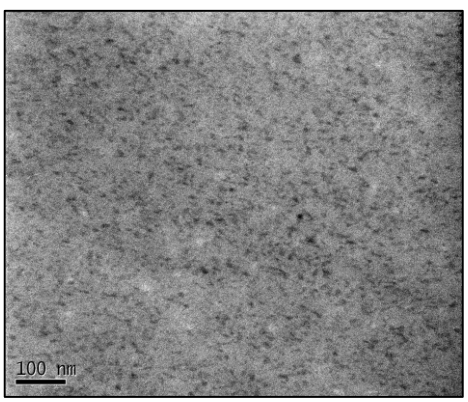

Figure 5. TEM image of a cryo-microtomed section of a 10 wt% Ti-based/**PM1** hybrid.

At a targeted 10 wt% TiO_2 loading, the behavior of the other *exo*-7-oxanorbornene monomers (**M2** through **M11**) was generally consistent with their respective hydrophilicities. Highly polar monomers, such as the alcohol adducts **M3** and **M4**, gave optically transparent materials, as did hybrids based on the sugar (**M5**) and captopril derivatives (**M10**). In contrast, more hydrophobic monomers such as the dodecyl (**M7**), benzyl (**M8**) and perfluoro (**M11**) derivatives exhibited significant phase separation and gave opaque composites. Interestingly, the charged cationic monomer (**M6**) also underwent phase separation during syntheses, suggesting that polarity may be less relevant than the ability to hydrogen bond.

It should be noted that the targeted TiO_2 loading plays a critical role in the phase separation behaviour of these hybrids. Even with the most hydrophilic, alcohol-functionalised, organic phases (poly**M3** and poly**M4**), a maximum of ca. 20 wt% Ti-based species could be added without gradual phase separation and agglomeration. Attempts were made to kinetically control this separation and lock the organic/inorganic phases in their relative positions by accelerating the polymerisation (by heating at 60 °C) and drying processes. While both approaches were fundamentally successful the hybrids gradually turned opaque over a period of 2-3 days due to macroscopic phase separation. While the exact cause of this gradual phase separation is unclear at this point, it is possible that there is sufficient migrational freedom associated with the inorganic domains, due to residual solvent (alcohols) and AcAc (both are difficult to remove completely from the resulting OINCs even with lengthy drying under vacuum) and/or the relatively low T_g's typical of the polymers derived from *exo*-7-oxanorbornenes.

This first series of studies highlighted a number of important features: i) there is a fundamental, but not ideal, compatibility between ROMP and Ti-based sol-gel chemistry that facilitates the ***concurrent*** preparation of OINCs; ii) In the case of **NBE**, the use of a β-diketone, such as AcAc, improves such fundamental compatibility and; iii) compatibility between the organic and inorganic phases can be further improved via substitution of **NBE** for a more polar monomer such as examples from the series of *exo*-7-oxanorbornenes shown in Figure 1. However, the targeted loading of titania still reached a limiting value of ca. 20 wt %.

An alternative, but complementary, approach to improve compatibility that addresses macroscopic phase separation involves the development of systems that facilitate covalent bonding between the polymeric organic and inorganic phases. The benefits of such an approach have been previously highlighted for obtaining high quality composite materials.[67]

Inspired by reports of other siloxy-containing monomers[68-73] we synthesized and employed 2-((3a*R*,7a*S*)-1,3-dioxo-3a,4,7,7a-tetrahydro-1*H*-4,7-epoxyisoindol-2(3*H*)-yl)ethyl 3-((3-(triethoxysilyl)propyl)thio)propanoate (**TES**, Figure 1) as a novel reactive (co)monomer. We previously reported the synthesis of **TES** and its attempted homogeneous solution ROMP with the Grubbs first generation initiator, $RuCl_2(PCy_3)_2CHPh$, but noted it resulted in the formation of crosslinked material due to condensation reactions associated with the pendent siloxy functional groups. However, when mixed with **TIP** and G2, not only does **TES** undergo ROMP but the siloxy groups also participate in hydrolysis and condensation reactions forming strong ***covalent*** links between the organic and inorganic phases. As a general observation, we note that the inclusion of **TES** as a reactive, polymerizable substrate, dramatically improved the homogeneity and performance of the hybrid OINC systems. Scheme 1 shows the proposed, idealized formation of covalent bonds between Si and Ti species in a co-condensation process. While we have not definitively proven the formation of covalent Si-O-Ti-type species we note numerous research groups have demonstrated

the formation of such hybrid groups in co-condensation process including those based on Si and Ti.[74-76]

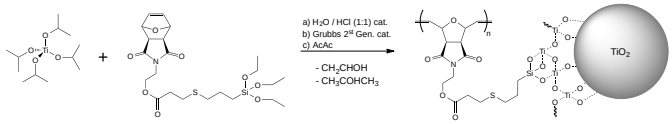

Scheme 1. Ideal formation of covalently linked organic/inorganic nanocomposites via simultaneous ROMP with a siloxy functional monomer and titania-based sol-gel condensation polymerization processes.

Consider first concurrent formulations comprised of **TES**, TIP, AcAc and **G2**, Table 1, entries 1-6. When employed as the sole organic polymerizable component it was possible to prepare hybrids containing up to **75** wt% Ti-based species while still yielding optically transparent materials with no sign of macroscopic phase separation. This crucially demonstrates one of the benefits of employing an organic monomer capable of undergoing both polymerization as well as co-condensing with the inorganic phase during the sol-gel process. Also, it is worth noting that the use of **TES** in conjunction with **TIP** not only gives a, presumably, covalently linked OINC but the inorganic phase is also, technically, a hybrid consisting of both Ti- and Si-based inorganic domains with the composite containing C-Si-O-Ti- type bonds. Perhaps most importantly, while we noted the advantageous use of AcAc as a compatibilizer for preparing transparent materials, in the case of **TES** it was possible to prepare an OINC containing 50 wt% Ti-based material without added AcAc, Figure 6.

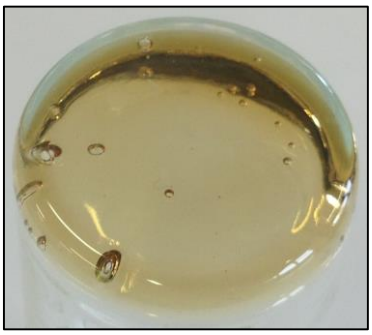

Figure 6. Digital picture of the OINC obtained from the simultaneous ROMP and titania sol-gel reactions of **TES** with **TIP** and Grubbs catalyst G2.

Table 1. Summary of simultaneous ROMP, mediated by the Grubbs G2 catalyst, and titania-based sol-gel process formulations conducted in the presence of AcAc

Entry	Organic component					Organic (wt %)	TiO_2 (wt %)
	ID	Monomer 1		Monomer 2			
		Functionality	mol %	ID	mol%		
1	**TES**	Triethoxysilane	100	-	-	90	10
2	**TES**	Triethoxysilane	100	-	-	80	20
3	**TES**	Triethoxysilane	100	-	-	70	30
4	**TES**	Triethoxysilane	100	-	-	60	40
5	**TES**	Triethoxysilane	100	-	-	50	50
6	**TES**	Triethoxysilane	100	-	-	25	75
7	**M1**	Butyl	50	**TES**	50	50	50
8	**M2**	Ethyl	50	**TES**	50	50	50
9	**M3**	Alcohol	50	**TES**	50	50	50
10	**M4**	Diol	50	**TES**	50	50	50
11	**M5**	Ac sugar	50	**TES**	50	50	50
12	**M6**	Cationic	50	**TES**	50	50	50
13	**M7**	Dodecyl	50	**TES**	50	50	50
14	**M8**	Benzyl	50	**TES**	50	50	50
15	**M9**	Thiazoline	50	**TES**	50	50	50
16	**M10**	Captopril	50	**TES**	50	50	50
17	**M11**	Perfluoro	50	**TES**	50	50	50
18	**POSS1**	Isobutyl	50	**TES**	50	50	50
19	**POSS2**	Disilanolisobutyl	50	**TES**	50	50	50

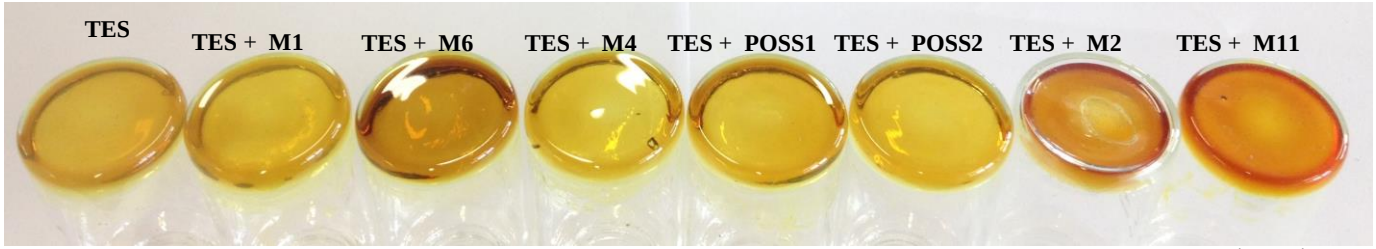

Figure 7. Representative digital photograph of a series of ONICs prepared with 50 wt% TiO_2 in the presence of AcAc and **TES** 50 wt%, image 1; (A) 50/50 **TES/M1**; (B) 50/50 **TES/M6**; (C) 50/50 **TES/M4**; (D) 50/50 **TES/POSS1**; (E) 50/50 **TES/POSS2**; (F) 50/50 **TES/M2** and (G) 50/50 **TES/M11**, demonstrating the optically transparent nature of the functional hybrid materials.

Characterization of the **TES** hybrids revealed interesting behaviour. In contrast to the optically transparent materials prepared at lower Ti loadings in the absence of **TES**, TEM of these samples appeared relatively featureless. Representative TEM images of 10, 30 and 50 wt% hybrids are shown in Figure 8.

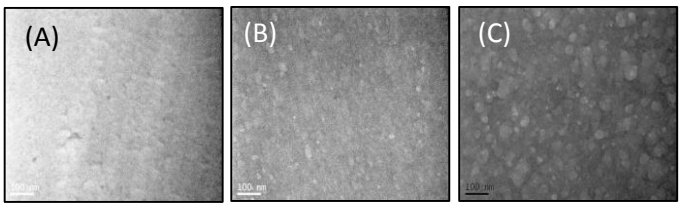

Figure 8. Representative TEM images of cryo-microtomed sections of **TES** hybrids with (A) 10, (B) 30 and (C) 50 wt% titania loadings.

Interestingly, none of the TEM images show the dark areas characteristic of evenly dispersed TiO_2 nanoparticles. This would suggest that near molecular homogeneity has been achieved in these **TES**-based hybrid materials. The clear presence of lighter regions in the 30 and 50 wt% samples has been attributed to nano-porosity as a result of residual isopropanol and AcAc. The relative density and size of these pores is consistent with the increasing concentration of porosigens associated with higher TiO_2 loadings. This also suggests that the Ti-species is in anamorphous state. This was qualitatively confirmed by Raman analysis of **TES** hybrids with 10, 30 and 50 wt% Ti-based species loadings. All spectra were essentially identical but all lacked signals associated with the common brookite, rutile and anatase forms of titania, see SI.

Small angle X-ray scattering was conducted on the covalently bound **TES** hybrids containing 10, 20, 30, 40 and 50 wt% Ti-based material, as well as a non-covalently bound **M1**/Ti-based control hybrid material, Figure 9.

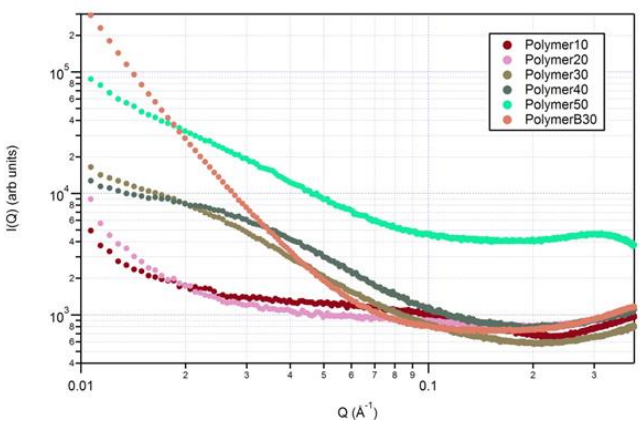

Figure 9. 1D SAXS data showing scattering intensity vs. Q for **TES**-based hybrids with 10, 20, 30, 40 and 50 wt% Ti-based and a **M1**/Ti-based material control.

For a general observation, the SAXS data indicates that the structures in these **TES**-based hybrids are non-trivial and the acquired data may be affected significantly by the presumed porosity associated with these materials, *vide supra*, with fitting of the data with known form/structure factor models[77] so far unsuccessful. Unfortunately, SEM of etched samples of the **TES** hybrids could not be performed due to their rapid dissolution in HF. It is believed that the inorganic Ti-based species acts as the crosslinking phase throughout these materials. Its removal by HF not only destroys the hybrid's network character but also hydrolyzes the siloxy pendants rendering the organic phase soluble in aqueous solutions. Qualitative swelling and thermal tests confirmed the acid degradable thermoset nature of these materials.

Preliminary DMA on **TES** hybrids containing 10, 20 and 30 wt% Ti-species showed an increase in T_g and modulus compared to a **TES** homopolymer control, Figure 10. While this general behaviour is consistent with inorganic composites and light crosslinking, the magnitudes of the increases were not proportional to the targeted TiO_2 levels. This result is likely related to porosity in the 20 and 30 wt% samples compromising the mechanical integrity of their test bars. A more thorough evaluation of the physical properties of these composites is underway and will be reported in the near future.

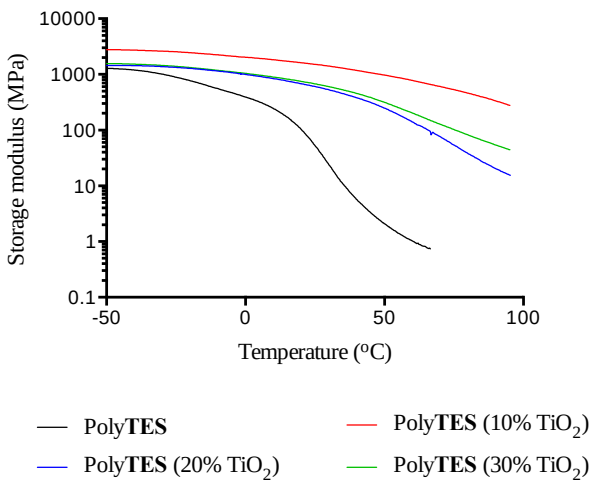

Figure 10. Dynamic mechanical analyses (DMA) of Poly(**TES**)/Ti-based hybrids showing an increase in glass transition temperature and modulus with covalently bound inorganic content.

Having noted the ability to include functional comonomers at 10 wt% in hybrid formulations and the ability of **TES** to yield transparent hybrids at high targeted titania loadings we next examined the ability to prepare novel functional hybrid materials containing 1:1 **TES**:*exo*-7-oxanorbornene comonomer at 50 wt%, entries 7-19 Table 1. All hybrids were prepared with G2 in the presence of AcAc. We believe that these represent the first known examples of covalently linked Si-Ti based OINCs containing a series of different functional groups as a means of further tuning physical properties. Figure 7 shows representative examples of the resulting copolymeric hybrid materials. In general these formulations resulted in the generation of optically transparent, albeit coloured, materials. The obvious exception to this was the formulation containing the perfluoro *exo*-7-oxanorbornene derivative **M11** (see Figure 7 far right) that yielded a material with a clear associated opaqueness. We are currently in the process of characterizing the physical properties of these new copolymeric/Si-Ti hybrid materials and will report the results in due course.

Conclusions

The simultaneous and *in situ* combination of ring-opening metathesis polymerization (ROMP) and titania-based sol-gel processes for the efficient synthesis of organic/inorganic hybrid materials is reported. The rapid rate and functional group tolerance of ROMP with the Grubbs' second-generation catalyst allows it to be readily paired with sol-gel chemistry. Hybrids containing targeted loadings of TiO_2 were prepared with commercially available norbornene as well as a range of functional *exo*-7-oxanorbornenes synthesized via thiol-Michael coupling chemistry. The degree of homogeneity of these materials was increased via the use of compatibilizing solvents, bidentate coordinating ligands and more polar monomers, leading to translucent composites containing 10-20 wt% of uniformly dispersed Ti-based nanoparticles. The subsequent introduction of a novel reactive triethoxysilane functionalized monomer (**TES**) resulted in a further step-change improvement in hybrid homogeneity. The resulting covalently bound systems appeared to be (near) molecularly homogeneous and up to 75 wt% of Ti species was readily incorporated without undergoing phase separation. This impressive performance was maintained even when the **TES** monomer was copolymerized with other *exo*-7-oxanorbornenes, allowing such materials to be functionalized with almost any chemical moiety. The **TES**-based hybrids behaved as acid degradable thermosets and exhibited excellent optical transparency, albeit coloured, which could be finely tuned by varying Ti content. Raman and TGA analysis suggested that rather than pure TiO_2 phases, the Ti-based species were likely oligomeric/polymeric Ti hydrates with the TI phases also existing in an amorphous state.

Acknowledgements

The authors acknowledge the facilities and technical assistance of the Electron Microscope Unit and Sigrid Fraser at the University of New South Wales. ABL would like to thank the Australian Research Council (ARC) for funding via the ARC-Discovery Projects program (DP110104391). He is also grateful for the award of a Future Fellowship (FT110100046). The CRC for Polymers is acknowledged for partial support of a scholarship for JvH.

Notes and references

[a] School of Chemical Engineering, UNSW Australia, University of New South Wales, Kensington, Sydney, NSW 2052, Australia.

Electronic Supplementary Information (ESI) is available, including FTIR spectra, additional SEM and TEM images and TGA and DMA traces. See DOI: 10.1039/b000000x/

1. D. Y. Godovsky, *Adv. Polym. Sci.*, 2000, 153, 163.
2. J. M. Garces, D. J. Moll, J. Bicerno, R. Fibiger and D. G. Mcleod, *Adv. Mater.*, 2000, 12, 1835.
3. M. Hoffman and S. Amberg-Schwab, *Mater. Res. Soc. Proc.*, 1998, 519, 309.
4. G. Kickelbick, *J. Sol-Gel Sci. Technol.*, 2008, 46, 281.
5. L. H. Lee and W. C. Chen, *Chem. Mater.*, 2001, 13, 1137.
6. F. X. Perrin, V. Nguyen and J. L. Vernet, *Polymer*, 2002, 43, 6159.
7. K. G. Sharp, *ACS Symp. Ser.*, 1995, 585, 163.
8. J. M. Yeh, C. J. Weng, K. Y. Huang, H. Y. Huang, Y. H. Yu and C. H. Yin, *J. Appl. Polym. Sci.*, 2004, 94, 400.
9. A. H. Yuwono, J. Xue, J. Wang, H. I. Elim, W. L. Ji and T. J. White, *J. Mater. Chem.*, 2003, 13, 1475.
10. W. C. Chen, S. J. Lee, L. H. Lee and J. L. Lin, *J Mater. Chem.*, 1999, 9, 2999.
11. G. Kickelbick, *Prog. Polym. Sci.*, 2003, 28, 83.
12. C. J. Brinker and G. W. Schere, *Sol-gel science*, Academic Press, San Diego, 1990.
13. K. H. Haas, *Handbook of organic-inorganic hybrid materials and nanocomposites*, American Scientific Publishers, Stevenson Ranch, USA, 2003.
14. G. Schottner, *Chem. Mater.*, 2001, 13, 3422.
15. A. B. Brennan, T. M. Miller and R. B. Vinocur, *ACS Symp. Ser.*, 1995, 585, 142.
16. E. J. A. Pope, M. Asami and J. D. Mackenzie, *J. Mater. Res.*, 1989, 4, 1018.
17. W. Apicatachutapan, R. B. Moore and K. A. Mauritz, *J. Appl. Polym. Sci.*, 1996, 62, 417.
18. P. L. Shao, K. A. Mauritz and R. B. Moore, *Chem. Mater.*, 1995, 7, 192.
19. J. M. Breiner and J. E. Mark, *Polymer*, 1998, 39, 5483.
20. Z. Ahmad, M. I. Sarwar and J. E. Mark, *J. Appl. Polym. Sci.*, 1998, 70, 297.
21. Z. Ahmad, M. I. Sarwar, J. Wang and J. E. Mark, *Polymer*, 1997, 38, 4523.
22. J. Wen and J. E. Mark, *Polym. J.*, 1995, 27, 495.
23. K. A. Mauritz and C. K. Jones, *J. Appl. Polym. Sci.*, 1990, 40, 1401.
24. W. T. Ferrar, B. K. Coltrain, C. J. T. Landry, V. K. Long, T. R. Molaire and D. E. Schildkraut, *ACS Symp. Ser.*, 1994, 572, 258.
25. B. K. Coltrain, W. T. Ferrar, C. J. T. Landry, T. R. Molaire and N. Zumbulyadis, *Chem. Mater.*, 1992, 4, 358.
26. L. Matejka, J. Plestil and K. Dusek, *J. Non-Cryst. Solids*, 1998, 226, 114.
27. L. Matejka, K. Dusek and J. Noga, *Wiley Polym. Networks Group Rev. Ser.*, 1998, I, 301.

28. L. Matejka, K. Dusek, J. Plestil, J. Kriz and F. Lednicky, *Polymer*, 1998, 40, 171.
29. M. X. Zhao, Y. P. Ning and J. E. Marl, *Ceram. Trans.*, 1991, 19, 891.
30. S. Wang, Z. Ahmad and J. E. Mark, *Polym. Bull.*, 1993, 31, 323.
31. C. J. T. Landry, B. K. Coltrain, J. A. Wessen, N. Zumbulyadis and J. L. Lippert, *Polymer*, 1992, 33, 1496.
32. Y. Chujo, *Curr. Opin. Solid State Mater. Sci.*, 1996, 1, 806.
33. T. Saegusa and Y. Chujo, *Makromol. Chem. Macromol. Symp.*, 1992, 64, 1.
34. T. Saegusa and Y. Chujo, *Makromol. Chem. Macromol. Symp.*, 1991, 51, 1.
35. R. Tamaki and Y. Chujo, *Appl. Organomet. Chem.*, 1998, 12, 755.
36. Y. Chujo and T. Saegusa, *Adv. Polym. Sci*, 1992, 100, 11.
37. K. A. Mauritz, *Mater. Sci. Engng.*, 1998, C6, 121.
38. P. L. Shao, K. A. Mauritz and R. B. Moore, *J. Polym. Sci. Part B: Polym. Phys.*, 1996, 34, 873.
39. Q. Deng, W. Jarrett, R. B. Moore and K. A. Mauritz, *J. Sol-Gel Sci. Technol.*, 1996, 7, 177.
40. Q. Deng, R. B. Moore and K. A. Mauritz, *Chem. Mater.*, 1995, 7, 2261.
41. N. Juangvanich and K. A. Mauritz, *J. Appl. Polym. Sci.*, 1998, 67, 1799.
42. G. Brusatin and G. D. Giustina, *J. Sol-Gel Sci. Technol.*, 2011, 60, 299.
43. R. Charvet and B. M. Novak, *Macromolecules*, 2001, 34, 7680.
44. B. L. Langsdorf, X. Zhou and M. C. Lonergan, *Macromolecules*, 2001, 34, 2450.
45. B. L. Langsdorf, X. Zhou and M. C. Lonergan, *Macromolecules*, 1999, 32, 2796.
46. M. G. Holland, V. E. Griffith, M. B. France and S. G. Desjardins, *J. Polym. Sci. Part A: Polym. Chem.*, 2003, 41, 2125.
47. D. A. Rankin and A. B. Lowe, *Macromolecules*, 2008, 41, 614.
48. D. A. Rankin, H. J. Schanz and A. B. Lowe, *Macromol. Chem. Phys.*, 2007, 208, 2389.
49. D. A. Rankin, S. J. P'Pool, H. J. Schanz and A. B. Lowe, *J. Polym. Sci. Part A: Polym. Chem.*, 2007, 45, 2113.
50. U. Frenzel and O. Nuyken, *J. Polym. Sci. Part A: Polym. Chem.*, 2002, 40, 2895.
51. C. W. Bielawski and R. H. Grubbs, *Prog. Polym. Sci.*, 2007, 32, 1.
52. S. Sutthasupa, M. Shiotsuki and F. Sanda, *Polym. J.*, 2010, 42, 905.
53. M. W. Ellsworth and B. M. Novak, *J. Am. Chem. Soc.*, 1991, 113, 2756.
54. O. Kir, N. Husing, D. Enke and W. H. Binder, *Macromol. Symp.*, 2010, 293, 67.
55. M. Liu, J. A. van Hensbergen, R. P. Burford and A. B. Lowe, *Polym. Chem.*, 2012, 3, 1647.
56. A. B. Lowe, M. Liu, J. A. van Hensbergen and R. P. Burford, *Macromol. Rapid. Commun.*, 2014, 35, 391.
57. M. Liu, B. H. Tan, R. P. Burford and A. B. Lowe, *Polym. Chem.*, 2013, 4, 3300.
58. M. Liu, R. P. Burford and A. B. Lowe, *Polym. Int.*, 2014, 63, 1174.
59. J. A. van Hensbergen, R. P. Burford and A. B. Lowe, *J. Polym. Sci. Part A: Polym. Chem.*, 2013, 51, 487.
60. J. A. van Hensbergen, R. P. Burford and A. B. Lowe, *Polym. Chem.*, 2014, 5, 5339.
61. J. A. van Hensbergen, T. W. Gaines, K. B. Wagener, R. P. Burford and A. B. Lowe, *Polym. Chem.*, 2014, 5, 6225-6235.
62. X. Chen and S. S. Mao, *Chem. Rev.*, 2007, 107, 2891-2959.
63. J. S. Pedersen, *J. Appl. Crystallogr.*, 2004, 37, 369.
64. L. van Lokeren, G. Maheut, F. Ribot, V. Escax, I. Verbruggan, C. Sanchez, J. Martins, M. Biesemans and R. Willem, *Chem. Eur. J.*, 2007, 13, 6957.
65. C. Sanchez, L. Rozes, F. Ribot, C. Laberty-Robert, D. Grosso, C. Sassoye, C. Boissiere and L. Nicole, *J. Non-Cryst. Solids*, 2010, 13, 3.
66. J. Zhang, S. Luo and L. Gui, *J. Mater. Sci.*, 1997, 32, 1469.
67. B. M. Novak, *Adv. Mater.*, 1993, 5, 422.
68. C. K. Chan and I. M. Chu, *Polymer*, 2001, 42, 6823.
69. R. O. R. Costa and W. L. Vasconcelos, *J Non-Cryst. Solids*, 2002, 304, 84.
70. J. Jang and H. Park, *J. Appl. Polym. Sci.*, 2002, 85, 2074.
71. C. Sanchez, G. J. D. A. A. Soler-Illia, F. Ribot and D. Grosso, *C. R. Chimie*, 2003, 6, 1131.
72. Y. Wei, D. Yang, D. J. Brennan, D. N. Rivera, Q. Zhuang, N. J. DiNardo and K. Qiu, *Chem. Mater.*, 1998, 10, 769.
73. Y. Wei, D. Yang, L. Tang and M. G. K. Hutchins, *J. Mater. Res.*, 1993, 8, 1143.
74. Y.-C. Song, Y. Hasegawa, S.-J. Yang and M. J. Sato, *J. Mater. Sci.*, 1988, 23, 1911.
75. J. Ren, Z. Li, S. Liu, Y. Xing and K. Xie, *Catal. Lett.*, 2008, 124, 185.
76. G. Phillip and H. Schmidt, *Non-cryst. Solids*, 1984, 63, 283.
77. B. Hammouda, *J. Appl. Crystallogr.*, 2010, 43, 716.